Peripheral Decoration of Multi-Resonance Molecules as a Versatile Approach for Simultaneous Long-Wavelength and Narrowband Emission

Yanyu Qi,[a,b,+] Weimin Ning, [c,+] Yang Zou, [a,*] Xiaosong Cao, [a] Shaolong Gong, [c,*] Chuluo Yang [a,*]

[a] Shenzhen Key Laboratory of Polymer Science and Technology, College of Materials Science and Engineering, Shenzhen University, Shenzhen 518060, People's Republic of China
E-mail: yangzou@szu.edu.cn; clyang@szu.edu.cn
[b] College of Physics and Optoelectronic Engineering, Shenzhen University, Shenzhen 518060, People's Republic of China
[c] Hubei Key Lab on Organic and Polymeric Optoelectronic Materials, Department of Chemistry, Wuhan University, Wuhan, 430072, People's Republic of China
Email: slgong@whu.edu.cn
[+] These authors contributed equally to this work.

Keywords: multi-resonance, thermally activated delayed fluorescence, organic light-emitting diodes, narrowband emission, color-purity

Abstract

High device efficiency and color-purity are the two essentials for high-quality organic light emitting diodes (OLEDs). Multi-resonance (MR) molecules show great potentials for high color-purity OLEDs due to their sharp emission bands. However, most MR molecules exhibit emission limited from deep-blue to green spectral region. Herein, through peripherally decorating MR emitter with electron donors, we demonstrated a new approach enabling the emission spectra of MR emitters red-shift while retaining narrowband emission. By manipulating the numbers and electron-donating abilities of the peripheries, the first narrowband yellow emitter with emission maxima of 562 nm and a full-width at half-maximum (FWHM) of 30 nm is

realized. Highly efficient OLEDs with external quantum efficiency of over 24% and excellent color purity are fabricated by employing these newly developed MR molecules as emitters.

1. Introduction

Developing highly efficient luminescent materials is highly demanded for the advancement of organic light emitting diodes (OLEDs). Among all the emitters, pure organic compounds are of the most promising materials due to their cost-effectiveness and highly variable chemical structures, allowing for harvesting excitons through various pathways.[1] One of the most extensively investigated emitters are the thermally activated delayed (TADF) materials based on the twisted donor-acceptor architecture.[2] In a TADF OLED, the small singlet-triplet energy gap (ΔE_{ST}) of the emitter allows both singlet (S1) and triplet (T1) excitons to be utilized *via* the reverse intersystem crossing (RISC) process, enabling a theoretical 100% internal quantum efficiency in the device. In this context, a few TADF emitters with external quantum efficiencies (EQEs) over 30% and emission colors varying from deep-blue to red have been reported.[3]

Apart from device efficiency, color-purity is also another important parameter that should be considered for high-quality displays. However, compared to the inorganic LEDs that exhibit narrowband emission with a full-width at half-maximum (FWHM) of ~20 nm,[4] most of the well-developed donor-acceptor type TADF OLEDs usually display broad emission band with FWHM over 50 nm. Such broadening of emission spectra is ascribed to the vibronic coupling between the ground state (S0) and singlet excited state (S1) as well as the structural relaxation of the S1 state for the conventional donor-acceptor type TADF emitters.[5] To address this issue, multi-resonance (MR) emitters have been invented by employing boron and nitrogen atoms into the rigid polycyclic aromatic hydrocarbon framework.[6] The multiple resonance effect can localize the highest occupied molecular orbital (HOMO) and lowest unoccupied molecular orbital (LUMO), and thus minimize the vibronic coupling and

vibrational relaxation of the emitter, sharpening the emission spectra and compressing FWHM. In addition, such localized HOMO and LUMO distribution with effective short range intramolecular charge transfer (ICT) of the MR emitters can also reduce the ΔE_{ST}, harvesting triplet excitons *via* facilitated RISC in the devices.

To date, a number of MR molecules have been developed by incorporating boron atoms[7] or carbonyl groups[8] into the fused planar triphenylamine frameworks. And OLEDs with high EQE of over 30% and narrow emission have been achieved by employing these MR molecules as emitters in OLEDs. Despite of the high efficiency and color purity, however, most of the currently developed MR emitters exhibit emission falls into deep-blue to green spectral region,[9] which inevitably limited their application for full-color displays. Although a handful of MR molecules with long wavelength emission have been reported,[10] some of these MR emitters are facing tedious synthetic issues with incredibly low yield, and some even suffer from spectra broadening.

One of the simplest and well-known MR molecules is **BNCz** (Scheme 1),[11] which exhibit narrowband bluish green emission with photoluminescence wavelength (λ_{PL}) of 481 nm. Several strategies have been developed for the derivation of **BNCz** to achieve long-wavelength emission. The first one is to introduce an electron acceptor onto the *para* position of the boron atom to increase the acceptor strength in the MR system. For example, Duan *et. al.* reported three green MR emitters by fluorobenzene substitution on the *para* position of boron in **BNCz**.[12] A pure green MR emitter with λ_{PL} of 522 nm and FWHM of 28 nm was also reported by fusing the aza-aromatics onto **BNCz**.[13] Another strategy is to install auxiliary carbazole moieties onto the *para* position of the nitrogen atom through the core to elevate the donor strength in the MR system. Wang *et. al.* reported a pure green MR emitter with λ_{PL} of 519 nm by installing an additional 3,6-di-*t*-butylcarbazole unit on the *para* position of nitrogen in **BNCz**.[14] And introducing two 3,6-di-*t*-butylcarbazole moieties led to a further red-shift of the spectrum, resulting greenish yellow emission with λ_{PL} of 549 nm.[10] In addition, peripheral conjugation extension was proved to cause the emission spectra

of MR molecules red-shift.[8c, 11] By integrating the "enhanced donor" and "peripheral conjugation extension" strategies together, we envisioned that the peripheral decoration of electron donating units onto the *para* position of nitrogen atoms on carbazole moieties in **BNCz** could give rise to the red-shifted emission. Herein, we designed a series of carbazole and diphenylamine end-capped **BNCz** molecules. Eventually, through versatilely changing the electron-donating ability and the number of the peripheral groups, the designed MR emitters **BN1-BN3** enabled the systematic color tuning of narrowband emissions from bluish-green (**BN1**) to green (**BN2**) and yellow (**BN3**). Highly efficient OLEDs with EQE_{max} beyond 24%, together with small FWHM were successfully fabricated based on these MR emitters.
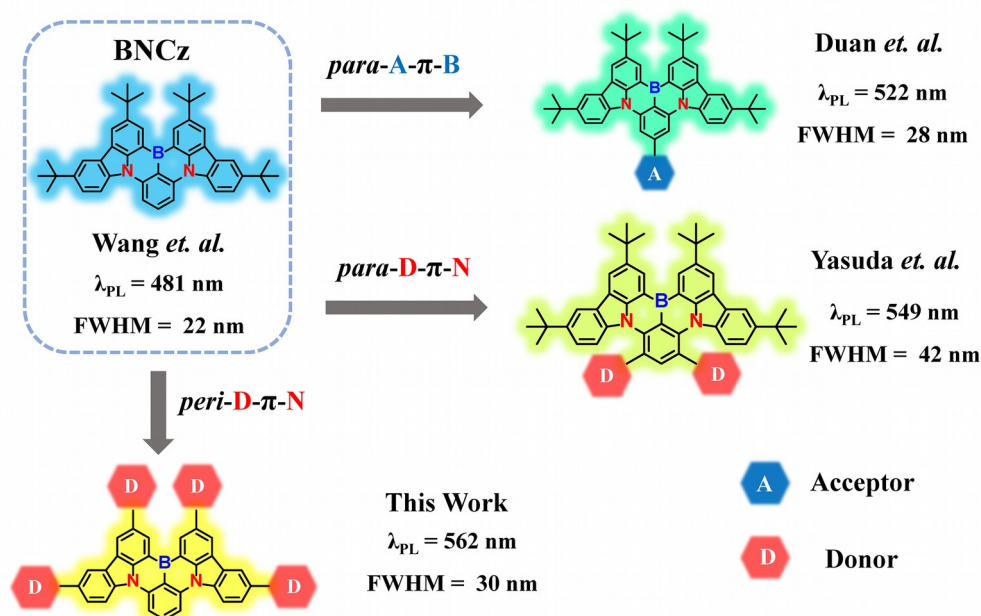

Scheme 1. Strategies for **BNCz** derivation toward long-wavelength emission.

2. Results and Discussion

2.1. Synthesis

The chemical structures of the designed molecules **BN1**, **BN2** and **BN3** were shown in Scheme 2. All the three molecules possessed a typical **BNCz** core, while **BN1** and **BN2** possessed unsymmetrical molecular structures with two of the *t*-butyl peripheries on carbazole being replaced by the weak electron donating carbazole (for

BN1) or strong electron donating diphenylamine (for **BN2**) moieties. Further fully replacement of the *t*-butyl peripheries in **BNCz** with diphenylamine gave the symmetrical molecule **BN3**. The synthesis of **BN1**-**BN3** was quite straightforward as depicted in Scheme S1 (see supporting information, SI), which involved nucleophilic substitution reactions between the commercially available carbazole derivatives and aryl fluoride, followed by the *t*-butyl lithium mediated borylation reactions. The reactions could be easily carried out on gram-scale and **BN1**-**BN3** were obtained in decent yields. Notably, owing to the rigid and planar framework, MR molecules free from solubilizing *t*-butyl groups usually exhibited poor solubilities in common organic solvents caused by strong aggregation. [8c] However, by integrating the rigid **BNCz** core with the flexible diphenylamine peripheries, **BN2** and **BN3** exhibited excellent solubilities in most organic solvents, allowing for facile purification and characterization. All the key intermediates and the final products were fully identified by ^{1}H, ^{13}C, ^{11}B NMR and high-resolution mass spectra (Figure S1-S20). In addition, as proved by thermogravimetric analysis (TGA, Figure S21), **BN1**-**BN3** all exhibited excellent thermal stability with decomposition temperature (T_d) of over 450 °C, enabling vacuum thermal deposition process for OLED fabrication.
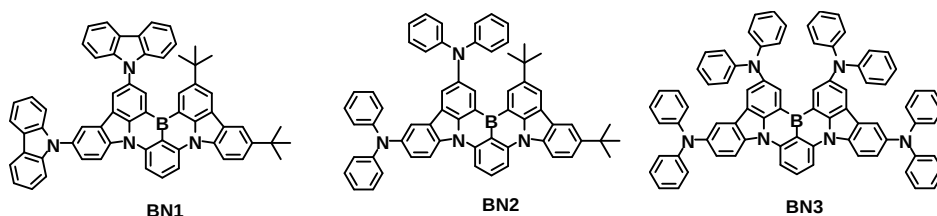
Scheme 2. Chemical structures of **BN1**, **BN2** and **BN3**.

2.2. Theoretical Calculation

Computational simulations based on the density functional theory (DFT) calculations were first conducted to validate the materials design. As illustrated in Figure 1, all three molecules shared similar molecular orbital distribution profile, in which the HOMOs showed significant contribution from the peripheral units. Replacing the carbazole end-cappers in **BN1** with strong electron-donating

diphenylamine moieties led to a remarkable shallowing of HOMO for **BN2** (-4.69 eV). Especially, with all the peripheral points of carbazole being fully end-capped with diphenylamine, **BN3** exhibited the shallowest HOMO of -4.66 eV. Moreover, the calculated E_g showed a clear trend of decrease with the increase of the numbers and the electron-donating abilities of peripheries. The calculated E_gs were 3.11, 2.87 and 2.75 eV for **BN1**, **BN2** and **BN3**, respectively, which were significantly smaller than that of **BNCz** (3.35 eV), corresponding to red-shifted emission spectra. In addition, large oscillator strengths (*f*) for the S1 excitation were predicted, indicating the efficient radiative decay and high PLQY for all the three molecules.
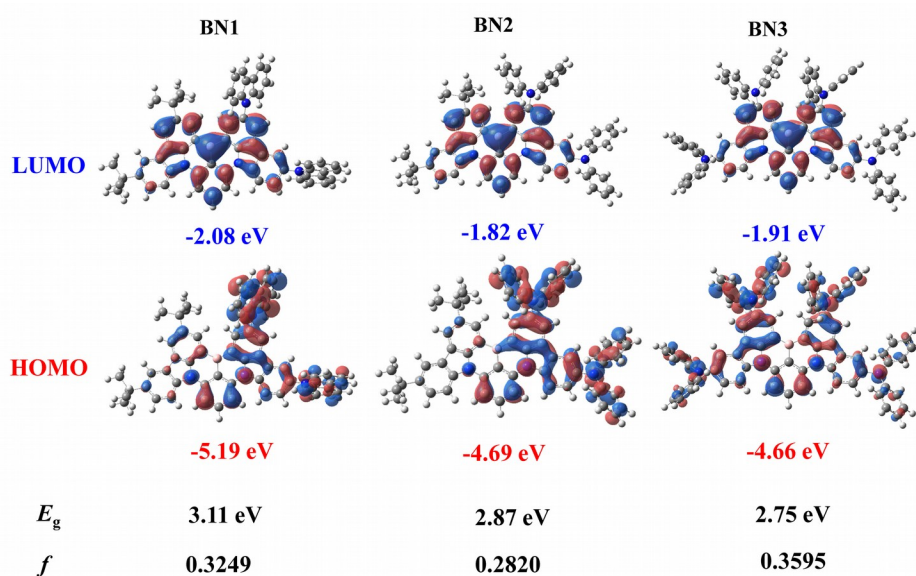

	BN1	BN2	BN3
LUMO	-2.08 eV	-1.82 eV	-1.91 eV
HOMO	-5.19 eV	-4.69 eV	-4.66 eV
E_g	3.11 eV	2.87 eV	2.75 eV
f	0.3249	0.2820	0.3595

Figure 1. The HOMO and LUMO energies, distributions, calculated energy gaps and oscillator strengths of **BN1**-**BN3**.

2.3. Electrochemical and Photophysical Properties

The predicted shallowing of HOMOs of **BN1**-**BN3** was convinced by the cyclic voltammetry (CV) results. As shown in Figure S22, **BN1** showed the onset potential of 0.29 V, while **BN2** and **BN3** displayed greatly lowered reversible half-wave potentials corresponding to the oxidation of the peripheral diphenylamine moieties. The calculated HOMOs were -5.09, -4.91 and -4.88 eV for **BN1**, **BN2** and **BN3**, respectively, the trend was well consistent with the theoretical prediction.

Photophysical properties were also investigated to correlate the theoretical calculations and the results were summarized in **Table 1**. In the UV-vis spectra (Figure 2a), all the three molecules revealed intense characteristic absorption band at 450-550 nm in toluene solution, which were assigned to ICT transitions. The absorption maxima (λ_{abs}) of ICT bands were gradually red-shifted from 478 nm (for **BN1**) to 503 nm (for **BN2**), and then 530 nm (for **BN3**), proving lowered S1 states as the numbers and the electron-donating abilities of the end-cappers increases.

BN1-BN3 all displayed bright emission with PLQYs of 98-99% in toluene solution (Figure 2b). And the emission maxima (λ_{em}) were gradually red-shifted from 496, to 534 and then 562 nm for **BN1**, **BN2** and **BN3**, respectively. Importantly, all three emitters exhibited narrowband emission with small FWHM and small Stokes shifts, meaning that the crucial MR promoted fluorescence were not interrupted by peripheral decoration. Notably, **BN3** displayed longer wavelength emission (λ_{em} of 562 nm) together with smaller FWHM of 30 nm, compared to the conventional MR molecule constructed by the "enhanced donor through the core" strategy (Scheme 1), which exhibited the λ_{em} of 549 nm and FWHM of 42 nm.[10] This finding clearly proved that the "peripheral decoration" approach could red-shift the emission of MR molecules without sacrificing the color purify. Additionally, all three emitters exhibited small ΔE_{ST}s of ~0.1 eV calculated from their fluorescence and phosphorescent spectra (Table 1, Figure S23).

Table 1. Physical data of **BN1**, **BN2** and **BN3**.

Emitter	T_g [°C]	λ_{abs}[a] [nm]	λ_{em}[a/b] [nm]	FWHM[a/b] [nm]	PLQY[a/b] [%]	HOMO[d] [eV]	LUMO[d] [eV]	S1 [eV]	T1 [eV]	ΔE_{st} [eV]
BN1	482	478	496/499	23/38	99/93	-5.09	-2.61	2.50	2.39	0.11
BN2	461	503	534/538	30/41	98/89	-4.91	-2.66	2.32	2.19	0.13
BN3	509	530	562/563	30/44	98/86	-4.88	-2.69	2.23	2.14	0.09

[a] Measured in toluene solutions (10^{-5} M) at 298K. [b] Measured in 1 wt.% doped in the mCBP. [d] HOMOs were calculated from CV; LUMO = HOMO + E_g^{opt}.

As shown in Figure 2c and summarized in Table 2, when doped in 3,3'-bis(carbazol-9-yl)biphenyl (mCBP) with the doping concentration of 1 wt.%, all three compounds displayed slightly red-shifted emission with spectra broadening due to the π-π interaction with the host, but high PLQYs remained as 86-93%. Thanks to their small ΔE_{ST}s, **BN1**-**BN3** exhibited a second-order exponential decay with nanosecond-scale prompt fluorescence and microsecond-scale delayed fluorescence as illustrated by the transient photoluminescence decay curves (Figure 2d). The fitted lifetimes of prompt (τ_p)/delayed (τ_d) fluorescence were 6.2 ns/68.6 μs, 7.1ns/107.6 μs and 6.3 ns/127.9 μs for **BN1**, **BN2** and **BN3**, respectively. When these emitters were employed as emitters for OLEDs, these large τ_ds should be considered carefully to avoid triplet-related quenching process.[15]
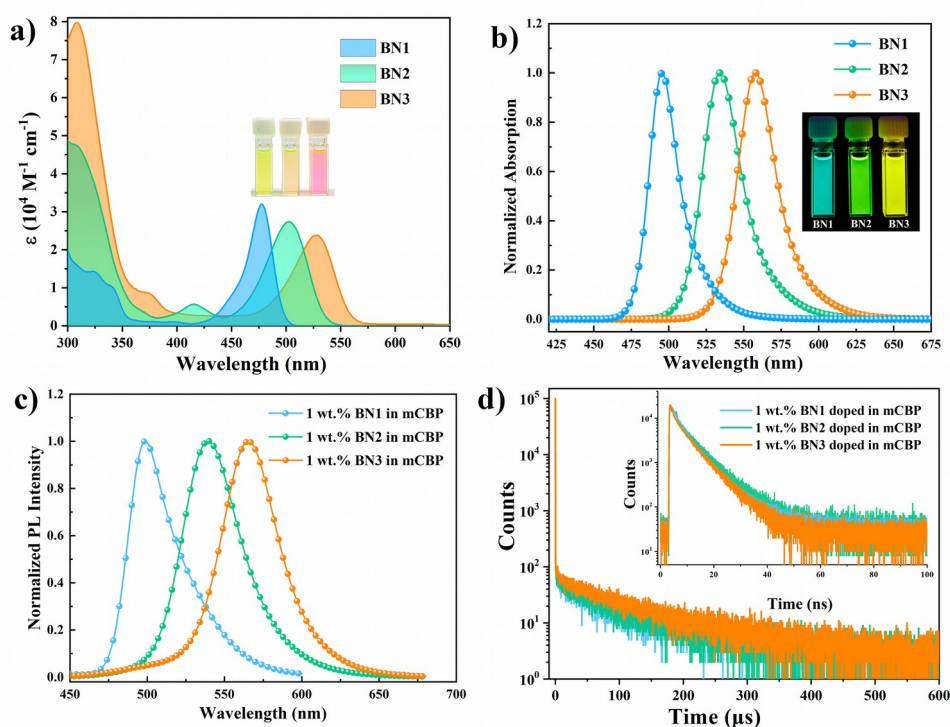

Figure 2. a) UV-vis spectra of **BN1**-**BN3** in toluene (10^{-5} M), b) fluorescence spectra of **BN1**-**BN3** in toluene (10^{-5} M), c) fluorescence spectra of **BN1**-**BN3** in doped film, d) transient photoluminescence decay curves of **BN1**-**BN3** in doped film under inert atmosphere (inset: prompt components).

Table 2. Physical data and kinetic parameters of 1 wt.% **BN1**-**BN3** doped in mCBP.

Emitter	$\Phi_{PL}{}^{a}$ (%)	$\Phi_{p}{}^{b}$ (%)	$\Phi_{d}{}^{b}$ (%)	$\tau_{p}{}^{c}$ (ns)	$\tau_{d}{}^{c}$ (μs)	$k_{r,S}{}^{d}$ $(10^{7}\ s^{-1})$	$k_{nr,S}{}^{d}$ $(10^{6}\ s^{-1})$	$k_{ISC}{}^{e}$ $(10^{7}\ s^{-1})$	$k_{RISC}{}^{e}$ $(10^{5}\ s^{-1})$
BN1	93	73	20	6.2	68.6	11.8	8.9	3.5	1.9
BN2	89	56	33	7.1	107.6	7.9	9.7	5.2	1.5
BN3	86	46	40	6.3	127.9	7.3	11.9	7.4	1.4

[a] Total photoluminescence quantum yield (Φ_{PL}); [b] Φ_{PL} contributions of the prompt component (p) and delayed (d) component; [c] lifetime of prompt and delayed fluorescence; [d] rate constant of radiative decay (k_r,s) and non-radiative decay (k_{nr},s) from S_1 to S_0 states; [e] intersystem crossing (ISC) and reverse intersystem crossing (RISC) rate constants.

2.4. Electroluminescence Performance

High PLQYs and narrowband emissions of these molecules inspired us to incorporate them into OLEDs as emitters. Initially, the simple doped OLEDs with the device configuration of ITO/HAT-CN (5 nm)/TAPC (30 nm)/mCP (10 nm)/EML (20 nm)/POT2T (10 nm)/TmPYPB (40 nm)/ Liq (1.5 nm)/Al (100 nm) were fabricated, in which dipyrazino[2,3-f:2′,3′-h]quinoxaline-2,3,6,7,10,11-hexacarbonitrile (HATCN) was served as a hole injection layer, 1,1-bis((di-4-tolylamino)phenyl)-cyclohexane (TAPC) and 1,3,5-tri(m-pyrid-3-ylphenyl)benzene (TmPyPb) were applied as hole- and electron-transport layers, while 1,3-di(9H-carbazol-9-yl)benzene (mCP) and 1,3,5-triazine-2,4,6-triyl)tris(benzene-3,1-diyl)(tris(diphenylphosphine oxide)) (POT2T) served as exciton-blocking layers (EBL). **BN1**-**BN3** were doped in mCBP host with the doping concentration of 1 wt.% to serve as EML.

As shown in Figure S24 and summarized in Table S1, all three devices demonstrated characteristic sharp electroluminescence (EL) peaks identical to the emitter's PL spectra. The maximum external quantum efficiencies (EQE$_{max}$s) were 17%, 20.7% and 21.4% for **BN1**, **BN2** and **BN3**-based devices, respectively, proving that both S1 and T1 excitons could be harvested by these MR emitters. However, these simple doped devices suffered from severe efficiency roll-offs. Taking **BN3**-based device for example, the EQE was only 5.3% at the brightness of 100 cd/m^2. The

severe efficiency roll-off was undoubtably ascribed to severe triplet-related quenching owing to the ultralong-lived triplet component of these MR emitters,[15a] as revealed by their transient photoluminescence decay curves.

Donor-acceptor-based exciplexes were well-known hosts for high-performance OLEDs due to the merits of decreased driving voltages, balanced charge transfer and 100% exciton harvesting capability.[16] To boost the device performances of OLEDs based on these MR emitters, exciplex based on mCBP:PO-T2T was selected as the host. As illustrated in Figure S25, the exciplex based on mCBP:PO-T2T showed clear TADF character, and its PL spectrum was well over-lapped with the absorption of **BN1**-**BN3**. Moreover, the doped film mainly showed emissions originated from the dopants with high PLQYs of 79%, 72% and 76% for **BN1**, **BN2** and **BN3**, respectively, indicating efficient energy transfer from the exciplex host to the MR emitters. Inspired by the good matching of the exciplex host and MR emitter dopants, the optimized OLEDs were further fabricated using the mCBP:POT2T:dopant structure as the EML, and the ratio of each component was set to 49.5:49.5:1, the device configuration, the chemical structures of the materials were shown in Figure 3, and the device results were summarized in Table 3.

All three OLEDs exhibited sharp EL spectra as shown in Figure 3c. **BN1**-based device showed bluish green emission with λ_{EL} of 506 nm and FWHM of 36 nm, and **BN2**-based device exhibited bright green emission with λ_{EL} of 545 nm and FWHM of 46 nm. Importantly, device based on **BN3** displayed yellow emission with Commission Internationale de l'Eclairage (CIE) of (0.47, 0.52), and a small FWHM of 43 nm. To the best of our knowledge, this was the first narrowband yellow OLED ever reported, and was also one of the few examples which possessed narrowband electroluminescnce of over 550 nm,[10] especially with such high device efficiency. Notably, with the help of the exciplex host, all three devices showed low turn voltage (V_{on}) of 3.0 V, brightness of over 5000 cd/m^2 and EQE$_{max}$ of over 24%. Particularly, the yellow OLED based on **BN3** showed an EQE$_{max}$ of 24.7% with suppressed efficiency roll-off (17.6% at 100 cd/m^2), a high maximum current efficiency (CE$_{max}$)

of 92.6 cd/A and a maximum power efficiency (PE_{max}) of 106.4 lm/W, which were remarkably improved compared to the mCBP-hosted devices.
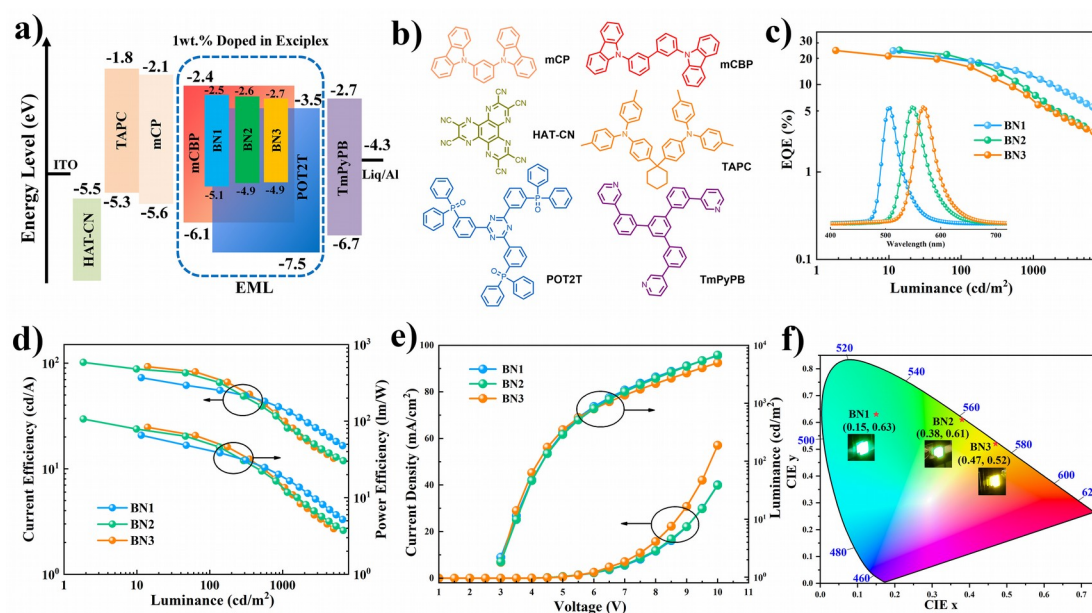

Figure 3. a) Device configuration and the energy level diagrams, b) chemical structures of the materials, c) EQE versus luminance curves (inset: the EL spectra), d) CE/PE versus luminance curves, e) luminescence and current density versus voltage characteristics, f) CIE coordinates and the images of the OLEDs

Table 3. Summary of the device data employing exciplex host.

Dopant	V_{on}[a] [V]	λ_{EL} [nm]	FWHM [nm]	L_{max}[b] [cd/ m²]	CE_{max}[c] [cd/ A]	PE_{max}[d] [lm/ W]	EQE[e] (%) @max/100/1000 cd m⁻²	CIE[f] (x, y)
BN1	3.0	506	36	6636	72.8	65.3	24.3/18.4/12.9	(0.15, 0.63)
BN2	3.0	545	46	6286	101.6	83.1	24.5/15.8/7.6	(0.38, 0.61)
BN3	3.0	568	43	5004	92.6	106.4	24.7/17.6/8.9	(0.47, 0.52)

[a] Turn-on voltage recorded at the brightness of 1 cd m⁻². [b] Maximum brightness. [c] maximum current efficiency. [d] Maximum power efficiency. [e] External quantum efficiency. [f] Commission Internationale de l'Eclairage, recorded at 7.0 V.

Conclusion

In summary, three new MR emitters **BN1**-**BN3** were designed and synthesized

through peripherally decorating the parent **BNCz** molecule with carbazole and diphenylamine moieties. The PL spectra of the emitters could be versatilely tuned from bluish-green to yellow by changing of the numbers and the electron-donating abilities of peripheries, meanwhile the property of narrowband emission was well retained. With diphenylamine fully decorated, **BN3** exhibited narrowband yellow emission with λ_{em} of 562 nm and FWHM of 30 nm. Accordingly, the exciplex-hosted OLED employing **BN3** as the emitter displayed an emission maxima of 568 nm and a small FWHM of 42 nm, which represent the first yellow OLED with narrowband emission ever reported. Moreover, the EQEmax of 24.7% was the highest for narrowband OLED with emission maxima over 550 nm. We believe this "peripheral decoration" approach would be enlightening for researchers to diversify the MR material library and further develop more colorful narrowband emitters.

Declaration of Competing Interest

The authors declare that they have no known competing financial interests or personal relationships that could have appeared to influence the work reported in this paper.

References

[1]   a) J. Partee, E. L. Frankevich, B. Uhlhorn, J. Shinar, Y. Ding, T. J. Barton, *Phys. Rev. Lett.* **1999**, *82*, 3673; b) W. J. Li, D. D. Liu, F. Z. Shen, D. G. Ma, Z. M. Wang, T. Feng, Y. X. Xu, B. Yang, Y. G. Ma, *Adv. Funct. Mater.* **2012**, *22*, 2797; c) D. Chaudhuri, E. Sigmund, A. Meyer, L. Rock, P. Klemm, S. Lautenschlager, A. Schmid, S. R. Yost, T. Van Voorhis, S. Bange, S. Hoger, J.

M. Lupton, *Angew. Chem. Int. Ed.* **2013**, *52*, 13449; d) S. Y. Byeon, D. R. Lee, K. S. Yook, J. Y. Lee, *Adv. Mater.* **2019**, *31*, 1803714.

[2]   a) Y. Tao, K. Yuan, T. Chen, P. Xu, H. Li, R. Chen, C. Zheng, L. Zhang, W. Huang, *Adv. Mater.* **2014**, *26*, 7931; b) M. Y. Wong, E. Zysman-Colman, *Adv. Mater.* **2017**, *29*, 1605444; c) Z. Yang, Z. Mao, Z. Xie, Y. Zhang, S. Liu, J. Zhao, J. Xu, Z. Chi, M. P. Aldred, *Chem. Soc. Rev.* **2017**, *46*, 915; d) Y. Liu, C. Li, Z. Ren, S. Yan, M. R. Bryce, *Nat. Rev. Mater.* **2018**, *3*, 18020.

[3]   a) T.-L. Wu, M.-J. Huang, C.-C. Lin, P.-Y. Huang, T.-Y. Chou, R.-W. Chen-Cheng, H.-W. Lin, R.-S. Liu, C.-H. Cheng, *Nat. Photonics* **2018**, *12*, 235; b) W. Zeng, H. Y. Lai, W. K. Lee, M. Jiao, Y. J. Shiu, C. Zhong, S. Gong, T. Zhou, G. Xie, M. Sarma, K. T. Wong, C. C. Wu, C. Yang, *Adv. Mater.* **2018**, *30*, 1704961; c) D. H. Ahn, S. W. Kim, H. Lee, I. J. Ko, D. Karthik, J. Y. Lee, J. H. Kwon, *Nat. Photonics* **2019**, *13*, 540; d) W. Li, B. Li, X. Cai, L. Gan, Z. Xu, W. Li, K. Liu, D. Chen, S. J. Su, *Angew. Chem. Int. Ed.* **2019**, *58*, 11301; e) Y. L. Zhang, Q. Ran, Q. Wang, Y. Liu, C. Hanisch, S. Reineke, J. Fan, L. S. Liao, *Adv. Mater.* **2019**, *31*, 1902368; f) W. Li, W. Li, L. Gan, M. Li, N. Zheng, C. Ning, D. Chen, Y.-C. Wu, S.-J. Su, *ACS Appl. Mater. Interfaces* **2020**, *12*, 2717.

[4]   a) V. L. Colvin, M. C. Schlamp, A. P. Alivisatos, *Nature* **1994**, *370*, 354; b) S. Coe, W. K. Woo, M. Bawendi, V. Bulovic, *Nature* **2002**, *420*, 800; c) S. I. Park, Y. Xiong, R. H. Kim, P. Elvikis, M. Meitl, D. H. Kim, J. Wu, J. Yoon, C. J. Yu, Z. Liu, Y. Huang, K. C. Hwang, P. Ferreira, X. Li, K. Choquette, J. A. Rogers, *Science* **2009**, *325*, 977; d) K. Zhang, D. Peng, K. M. Lau, Z. J. Liu, *J. Soc. Inf. Disp.* **2017**, *25*, 240.

[5]   F. Santoro, A. Lami, R. Improta, J. Bloino, V. Barone, *J. Chem. Phys.* **2008**, *128*, 224311.

[6]   a) T. Hatakeyama, K. Shiren, K. Nakajima, S. Nomura, S. Nakatsuka, K. Kinoshita, J. Ni, Y. Ono, T. Ikuta, *Adv. Mater.* **2016**, *28*, 2777; b) X. Liang, Z. P. Yan, H. B. Han, Z. G. Wu, Y. X. Zheng, H. Meng, J. L. Zuo, W. Huang,

Angew. Chem. Int. Ed. **2018**, *57*, 11316; c) K. Matsui, S. Oda, K. Yoshiura, K. Nakajima, N. Yasuda, T. Hatakeyama, *J. Am. Chem. Soc.* **2018**, *140*, 1195; d) Y. Kondo, K. Yoshiura, S. Kitera, H. Nishi, S. Oda, H. Gotoh, Y. Sasada, M. Yanai, T. Hatakeyama, *Nat. Photonics* **2019**, *13*, 678; e) N. Ikeda, S. Oda, R. Matsumoto, M. Yoshioka, D. Fukushima, K. Yoshiura, N. Yasuda, T. Hatakeyama, *Adv. Mater.* **2020**, *32*, 2004072; f) J. M. Teng, Y. F. Wang, C. F. Chen, *J. Mater. Chem. C* **2020**, *8*, 11340.

[7]   S. Madayanad Suresh, D. Hall, D. Beljonne, Y. Olivier, E. Zysman-Colman, *Adv. Funct. Mater.* **2020**, *30*, 1908677.

[8]   a) Y. Yuan, X. Tang, X.-Y. Du, Y. Hu, Y.-J. Yu, Z.-Q. Jiang, L.-S. Liao, S.-T. Lee, *Adv. Opt. Mater.* **2019**, *7*, 1801536; b) S.-N. Zou, C.-C. Peng, S.-Y. Yang, Y.-K. Qu, Y.-J. Yu, X. Chen, Z.-Q. Jiang, L.-S. Liao, *Org. Lett.* **2021**, *23*, 958; c) D. Hall, S. M. Suresh, P. L. dos Santos, E. Duda, S. Bagnich, A. Pershin, P. Rajamalli, D. B. Cordes, A. M. Z. Slawin, D. Beljonne, A. Kohler, I. D. W. Samuel, Y. Olivier, E. Zysman-Colman, *Adv. Opt. Mater.* **2020**, *8*, 1901627; d) H. Min, I. S. Park, T. Yasuda, *Angew. Chem. Int. Ed.* **2021**, DOI: 10.1002/anie.202016914.

[9]   a) S. Oda, B. Kawakami, R. Kawasumi, R. Okita, T. Hatakeyama, *Org. Lett.* **2019**, *21*, 9311; b) H. Lee, D. Karthik, R. Lampande, J. H. Ryu, J. H. Kwon, *Front. Chem.* **2020**, *8*, 373.

[10]   M. Yang, I. S. Park, T. Yasuda, *J. Am. Chem. Soc.* **2020**, *142*, 19468.

[11]   Y. C. Xu, Z. Cheng, Z. Q. Li, B. Y. Liang, J. X. Wang, J. B. Wei, Z. L. Zhang, Y. Wang, *Adv. Opt.Mater.* **2020**, *8*, 1902142.

[12]   Y. Zhang, D. Zhang, J. Wei, Z. Liu, Y. Lu, L. Duan, *Angew. Chem. Int. Ed.* **2019**, *58*, 16912.

[13]   Y. Zhang, D. Zhang, J. Wei, X. Hong, Y. Lu, D. Hu, G. Li, Z. Liu, Y. Chen, L. Duan, *Angew. Chem. Int. Ed.* **2020**, *59*, 17499.

[14]   Y. Xu, C. Li, Z. Li, Q. Wang, X. Cai, J. Wei, Y. Wang, *Angew. Chem. Int. Ed.* **2020**, *59*, 17442.

[15]   a) N. Notsuka, R. Kabe, K. Goushi, C. Adachi, *Adv. Funct. Mater.* **2017**, *27*,

1703902; b) K. H. Lee, J. Y. Lee, *Org. Electron.* **2019**, *75*, 105377; c) J. H. Smit, J. H. M. van der Velde, J. Huang, V. Trauschke, S. S. Henrikus, S. Chen, N. Eleftheriadis, E. M. Warszawik, A. Herrmann, T. Cordes, *Phys. Chem. Chem. Phys.* **2019**, *21*, 3721.

[16]   Q. Wang, Q.-S. Tian, Y.-L. Zhang, X. Tang, L.-S. Liao, *J. Mater. Chem. C* **2019**, *7*, 11329.

Table of Contents

Peripheral Decoration of Multi-Resonance Molecules as a Versatile Approach for Simultaneous Long-Wavelength and Narrowband Emission

Yanyu Qi,[a,b,+] Weimin Ning, [c,+] Yang Zou, [a,*] Xiaosong Cao, [a] Shaolong Gong, [c,*] Chuluo Yang [a,*]

This work demonstrates a versatile approach by peripheral decoration of multi-resonance molecules, which enables emission spectra red-shift while remains narrowband emission. Fully decorating the parent **BNCz** molecules with diphenylamine gives the first narrowband yellow emissive MR emitter with emission maxima of 562 nm. Electroluminescence devices employing these MR emitters reveal narrowband emission with high external quantum efficiency of over 24%.